ACTA
AMAZONICA

http://dx.doi.org/10.1590/1809-4392202103682

ORIGINAL ARTICLE

The role of topographic-derived hydrological variables in explaining plant species distributions in Amazonia

Gabriel M. MOULATLET[1,7*], Camilo D. RENNÓ[2], Fernando O. G. FIGUEIREDO[3], Kalle RUOKOLAINEN[1,4], Lise BANON[2], Thaise EMILIO[5], Henrik BALSLEV[6], Hanna TUOMISTO[1]

[1] University of Turku, Department of Biology, Turku, Finland
[2] Instituto Nacional de Pesquisas Espaciais, Divisão de Observação da Terra e Geoinformática, São José dos Campos, São Paulo, Brazil
[3] Instituto Nacional de Pesquisas da Amazonia, Manaus, Amazonas, Brazil
[4] University of Turku, Department of Geography and Geology, Turku, Finland
[5] Universidade Estadual de Campinas, Instituto de Biologia, Programa Nacional de Pós-Doutorado (PNPD), Programa de Pós-Graduação em Ecologia, Campinas, São Paulo, Brazil
[6] Aarhus University, Department of Biology, Section Ecoinformatics and Biodiversity, Aarhus, Denmark
[7] Instituto de Ecología A.C., Red de Biología Evolutiva, Xalapa, Veracruz, Mexico
* Corresponding author: mandaprogabriel@gmail.com; https://orcid.org/0000-0003-2571-1207

ABSTRACT

In Amazonian terra-firme non inundated forests, local floristic composition and species occurrence are explained by water availability as determined by topographic conditions. Topographic complexity can render these conditions quite variable across the landscape and the effects on plant ecological responses are difficult to document. We used a set of topographically defined hydrological metrics to evaluate community composition and single-species responses of four plant groups [pteridophytes (ferns and lycophytes), Melastomataceae, palms (Arecaceae) and Zingiberales] to topographic conditions in the middle Juruá River region, in western Brazilian Amazonia. The area spans two geological formations (Içá and Solimões) with contrasting topography. River terraces are also found along the main rivers in the area. Local topographic conditions were approximated by height above the nearest drainage (HAND), slope, and Strahler´s drainage order, all obtained from a SRTM digital elevation model (DEM). Data were analyzed using linear and generalized linear mixed models and regression trees. HAND was most successful in explaining floristic composition for all plant groups, except for Melastomataceae, and was more important in the hilly Içá formation than in the Solimões. Individual occurrences of 57% species were predicted by at least one of the topographic variables, suggesting a marked habitat specialization along topographic gradients. For these species, response models using SRTM-DEM-derived variables gave similar results than models using field-measured topography only. Our results suggest that topographical variables estimated from remote sensing can be used to predict local variation in the structure of plant communities in tropical forests.

KEYWORDS: DEM, geological formations, HAND, vegetation mapping

O papel de variáveis hidrológicas derivadas da topografia em explicar a distribuição de espécies de plantas na Amazônia

RESUMO

Nas florestas de terra firme não inundáveis da Amazônia, a composição florística e a ocorrência de espécies podem ser explicadas pela disponibilidade hídrica relacionada com a topografia. Dada a complexidade topográfica, a disponibilidade de água pode ser bastante variável e seus efeitos na resposta das plantas, difícil de documentar. Neste estudo avaliamos as respostas individuais de espécie de quatro grupos de plantas [pteridófitas (samambaias e licófitas), Melastomataceae, palmeiras (Arecaceae) e Zingiberales] às condições topográficas na região do médio Rio Juruá, no oeste da Amazônia brasileira. A área abrange duas formações geológicas (Içá e Solimões) com topografias contrastantes. Terraços fluviais também são encontrados ao longo dos rios principais. As condições topográficas foram medidas usando a altura acima da drenagem mais próxima (HAND), declividade e ordem de drenagem de Strahler, todas obtidas a partir de um modelo digital de elevação SRTM-DEM. Os dados foram analisados usando modelos lineares generalizados mistos e árvores de regressão. HAND foi a principal variável explicativa da composição florística para todos os grupos de plantas, exceto Melastomataceae, tendo maior efeito na formação Içá do que na Solimões. Ocorrências individuais de 57% das espécies foram explicadas por pelo menos uma das variáveis, sugerindo uma especialização marcada de habitat ao longo de gradientes topográficos. Para essas espécies, modelos usando variáveis derivadas do SRTM-DEM deram resultados semelhantes aos modelos usando apenas a topografia medida em campo, o que indicam que variáveis topográficas derivadas do SRTM-DEM podem ser usadas para prever variações locais na estrutura de comunidades de plantas em florestas tropicais.

PALAVRAS-CHAVE: DEM, formações geológicas, HAND, mapeamento de vegetação

CITE AS: Moulatlet, G.M.; Rennó, C. D.; Figueiredo, F.O.G.; Ruokolainen, K.; Banon, L.; Emilio, T.; Balslev, H.; Tuomisto, H. 2022. The role of topographic-derived hydrological variables in explaining plant species distributions in Amazonia. *Acta Amazonica* 52: 218-228.

INTRODUCTION

Answering general questions on plant species distribution in Amazonia has been hampered by the lack of detailed information on how the species niche is constrained by environmental conditions (Tuomisto *et al.* 2019). In particular, soil nutrient concentration and water availability are important determinants of plant species distributions and floristic composition. Several studies show that occurrence and abundance of Amazonian plant species vary along gradients of soil nutrient concentration (Ca, Mg, K, Na) and available phosphorus (Tuomisto *et al.* 1998; 2016; Costa *et al.* 2005; Higgins *et al.* 2011; Zuquim *et al.* 2012; Baldeck *et al.* 2016; Cámara-Leret *et al.* 2017). Floristic composition also varies along local topographical gradients from hilltops to valley bottoms (Tuomisto *et al.* 1995; Tuomisto and Poulsen 2000; Poulsen *et al.* 2006) because topographic units (i.e., bottomlands, slopes and hilltops or plateaus) differ substantially in water availability (Nobre *et al.* 2011). As topography and soil nutrients can be correlated due to topographically controlled soil formation, plant species may respond to both, as they are exposed to geochemical sedimentary layers with different nutrient concentration at different topographical positions (Tuomisto and Ruokolainen 1994, Vormisto *et al.* 2004; Baldeck *et al.* 2013; Chauvel *et al.* 1987; Osher and Buol 1998; Chadwick and Asner 2016). Yet floristic changes in topographic gradients are less obvious than soil gradients due to the absence of a metric that allows cross-scale comparisons of topographic conditions.

In Amazonia large areas are seasonally inundated on the river floodplains, which makes them ecologically and floristically distinct from areas of terra firme (Campbell *et al.* 1986; Balslev *et al.* 1987; Gentry 1988; Wittmann *et al.* 2013). In terra firme forests, environmental gradients are often defined by topographic variation. Topography, in turn, is a proxy for several environmental conditions that are important determinants of species distribution (Vormisto *et al.* 2004; Moeslund *et al.* 2013). Especially drainage has a clear relation to local topography, determining water availability as lower areas have higher water availability due to proximity to the water table and due to runoff of rainwater from higher areas (Fan *et al.* 2019). These characteristics make it possible to use topography as a practical surrogate of water availability on the terrain (Haitjema and Mitchell-Bruker 2005; Rennó *et al.* 2008; Costa *et al.* 2022).

Direct measurements of soil water availability or water table depth are time-consuming and very much affected by weather conditions during and just before measurement. In fact, few studies on plant species distribution in Amazonian terra firme have correlated such measurements with plant species distribution (e.g., Jirka *et al.* 2007; Guimaraes *et al.* 2021). Instead, topographic variation has been used as a surrogate for local hydrological conditions when addressing changes in local floristic composition, either by measuring topographic variation in the field (Tuomisto *et al.* 1995; Tuomisto and Poulsen 2000; Drucker *et al.* 2008; Costa *et al.* 2009), or by making a simple (and subjective) classification of topographic units (e.g. plateaus, slopes and valleys) into hydromorphic environments (Kahn and de Castro 1985; Svenning 1999; Drucker *et al.* 2008). In the absence of field measured topography, topographic metrics derived from digital elevation models (DEMs) have been applied as determinants of floristic composition. Out of these metrics, the algorithm HAND (height above the nearest drainage, Rennó *et al.* 2008) has stood out as a proxy for topographically defined hydrological conditions in terrains with relatively homogeneous soil conditions (Moulatlet *et al.* 2014; Schietti *et al.* 2014), but in terrains with highly heterogeneous soil conditions, its applicability has not been evaluated yet.

Remote sensing data may help to fill the gap in environmental information needed to map species distribution at different scales (Rocchini *et al.* 2016). However, the association of environmental processes with species distribution from local to regional scales needs remote sensing data coupled with data on species occurrences that covers a large part of the environmental heterogeneity (Tuomisto *et al.* 2019). We used an extensive dataset of field measured topography in the western Brazilian Amazon to assess the ability of HAND and two other DEM-derived topographic metrics (i.e., the estimated topographic conditions) as proxies of local hydrological conditions to explain floristic composition and plant species distribution across two geological formations. We focused on four plant groups (pteridophytes, palms, Melastomataceae and Zingiberales) and addressed community and individual species responses to both field and DEM-derived topography. We specifically asked: i) whether species distributions of the different plant groups can be explained by the estimated topographic conditions; ii) what is the response magnitude and direction (i.e., positive, or negative) of individual species to the estimated topographic conditions; and iii) to which degree the species responses can be compared to local topographic measurements, i.e., if DEM-derived variables can replace topographic field measurements as useful metrics to be associated with floristics.

MATERIAL AND METHODS

Study Area

The study was conducted in western Amazonia in Brazil along the rivers Juruá and Tarauacá, with field sampling extending across 500 km (Figure 1). The study area is covered by continuous rainforest at an elevation range of 65–200 m.a.s.l. Mean annual rainfall is 2200 mm and annual mean temperature is 27 °C, with temperatures as low as 15 ºC occurring during annual cold spells (Karger *et al.* 2017). The area is in a complex geological setting. The Içá and Solimões

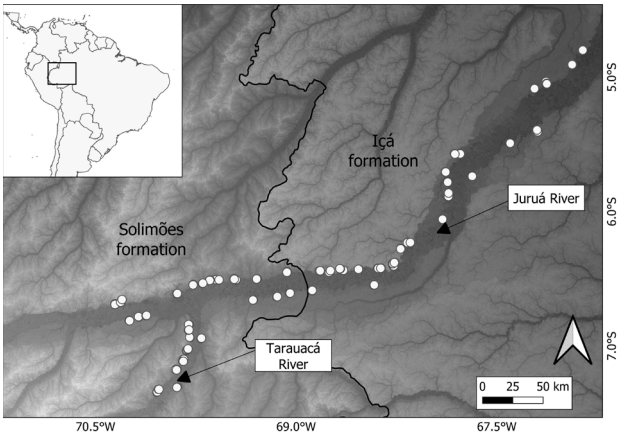

Figure 1. Location of the study area in western Amazonia (Brazil). Sampling transects (white dots) were located along the rivers Juruá and Tarauacá. The dark line shows the limit between the Içá and Solimões formations, as determined by Higgins *et al.* (2011). Background shading represents elevation differences as indicated by the SRTM DEM. Lighter areas are of higher elevation than darker areas.

formations underlie most of the terrain, and river terraces are present along both rivers (Table 1). The Içá Formation consists of relatively nutrient poor and loamy to sandy sediments deposited during the Pliocene to Pleistocene, and the terrain is typically steep and hilly (Hoorn and Wesselingh 2011). The Solimões Formation consists of relatively nutrient rich clay sediments deposited under semi-marine or lacustrine conditions during the Miocene (Hoorn and Wesselingh 2011), and the topography is generally flat or undulating. Alluvial terraces extend along the main rivers that consist of sediments of varying textures in abandoned floodplains due to lateral migration of the river channel. The differences in soil nutrient concentration of these geological formations have already been shown to explain the main gradients in plant species composition (Higgins *et al.* 2011; Tuomisto *et al*. 2016).

Sampling design

A total of 71 line transects were established between March and June of 2012. The transects were placed in sites where Landsat image interpretation suggested that primary terra-firme forest was sufficiently close to the river to be reached by foot and inventoried within one day of trekking. The exact location and compass bearing of transects were chosen to include as much as possible of the local topographical heterogeneity. Each transect was 500 m long and consisted of 20 subunits of 25 m x 5 m. The topography of each transect was measured using a clinometer at 20–25-m intervals and whenever there was a significant change in slope. When transects were so flat that the measurement error was estimated to be larger than the actual slope of the terrain, topography was not measured, and the slope was assumed to equal zero. Transect coordinates were obtained in the field with a hand-held GPS.

Floristic data

We use the same floristic data as Tuomisto *et al.* (2016). Floristic inventories were made at the 25-m subunit resolution within each transect. For pteridophytes, we registered all individuals with at least one green leaf (leafy stem in the case of lycophytes) longer than 10 cm, including epiphytes, hemiepiphytes and climbers if they had such leaves less than two meters above ground. All Melastomataceae individuals with post-cotyledon leaves were included. All Zingiberales individuals with a minimum height of 5 cm were recorded and, in the case of clonal species, bunches of leaves separated by at least 20 cm were considered as separate individuals. All palm individuals higher than 5 cm were included, but palm seedlings that could not be identified to species level were excluded. Each ramet in a clonal or colonial species was counted as an individual. Representative voucher specimens were deposited in the herbaria of the University of Turku, Finland (pteridophytes and Melastomataceae), University of Aarhus, Denmark (palms), Instituto Nacional de Pesquisas da Amazônia, Brazil (palms and Zingiberales) and Instituto de Botanica – Universidade de São Paulo, Brazil (pteridophytes and Melastomataceae). Pteridophytes and Melastomataceae were inventoried in all 71 transects, palms in 40 and Zingiberales in 39 (Supplementary Material, Table S1).

Topographic data

To place all transects on the same elevational and topographical framework, we used the digital elevation model (DEM) of the Shuttle Radar Topographic Mission (SRTM) with resolution of 1 arc sec (~30 m at the equator) to obtain elevation data for each 25-m subunit. Before extracting the SRTM elevation values for each subunit, we compared the SRTM-derived topographic profile of each transect with the corresponding field-measured true profile. This was done to account for possible errors associated with the measurements of transect coordinates. If there was a mismatch, we adjusted transect georeferencing to obtain the best possible match of

Table 1. Environmental variables measured along transects set in each of three geological settings along the middle Juruá River (western Brazilian Amazon). Mean (minimum - maximum) values are shown.

Geological setting	Number of transects	Field-measured topography (m)	HAND (m)	Slope (%)	SRTM (m)	Maximum Strahler's drainage order
Içá Formation	15	14.69 (0 - 40.62)	12.71 (0.02 - 43.32)	5.42 (1.21-7.94)	155.56 (124.01 - 192.4)	5
Solimões Formation	23	8.67 (0 - 28.74)	8.21 (0.02 - 31.64)	3.74 (0-8.6)	154.38 (125.26 - 187.76)	4
River terraces	33	4.68 (0 - 16.73)	3.43 (0 - 19.7)	2.73 (0-7.15)	119.26 (69 - 174.55)	6

the SRTM profile with the field-measured topography using an algorithm that optimized the search for initial points with similar topographic profiles. The initial SRTM profiles were based on the field-measured coordinates at the start and end points of each transect, as transects were assumed to be straight lines without major deviations. The coordinate correction procedure iteratively recalculated the start and end coordinates of each transect, such that the sum of the squared differences between field-measured and SRTM-derived topographic profiles were minimized. This was done with the constraint that the new coordinates could not be displaced by more than two SRTM pixels (approximately 60 m) from the original coordinates. In the next step, the new coordinates were used to assign coordinates for each 25-m subunit and to extract SRTM elevation values by bilinear interpolation. With this procedure, we had SRTM-derived topographic profiles that matched the topographies measured in the field. For five of the 71 transects (transects 780, 794, 806, 807 and 808) our algorithm failed to match with the topographic profiles within the range of 60 m and, therefore, these transects were not included in the final analysis. The R code for the algorithm can be found at (https://github.com/gamamo/Jurua-Hydro).

Based on the adjusted transect georeferencing, we calculated a single HAND value for each transect subunit. HAND is a topographic measure that equals the vertical distance (in meters) between a point of interest and the nearest watercourse (or point where the water table is assumed to be near the surface). Low HAND values correspond to moister sites close to the water table, and high HAND values to drier sites further above the water table. Since HAND is independent of absolute elevation, its values are comparable over large areas. We calculated HAND using a remote sensing-based algorithm developed by Rennó *et al*. (2008) which combines the STRM-DEM with a drainage network. We set as drainage network for each geological formation the one produced by Banon (2013), which uses a decision tree based on several topographic attributes extracted from the SRTM-DEM, including accumulated area, slope and curvatures, to determine the best drainage network for a given area.

To complement the HAND estimates, we derived two other topographic variables related to the local hydrological conditions, namely slope and stream order of the nearest drainage (according to Strahler 1957) from the SRTM-DEM. Slope is related to the overland and subsurface flow of water, and therefore it affects potential soil moisture, which is generally higher on gentler slopes. Strahler's stream order is an estimate of the size of a water channel based on the same drainage network that was generated to calculate the HAND. In Amazonian forests, water table depth varies not only along topographic profiles, but also according to the distance to rivers of different drainage orders. Low values of Strahler`s drainage order are found often near the headwaters and indicate intermittent waterflow dominated by ground water streamflow. Strahler`s drainage order increases downstream and larger values indicate more continuous waterflow, the magnitude of which depends on the interplay between infiltration from large rivers and ground water depth (Miguez-Macho and Fan 2012).

Data Analysis

The floristic responses (community-level analysis) to the topographic predictors were assessed using regression models developed for each of the four plant groups separately. To use community data as the response variable, we reduced the dimensionality of the data through NMDS (non-metric multidimensional scaling) to two dimensions. A floristic dissimilarity matrix for each NMDS was calculated using the extended Sørensen dissimilarity. This is based on the classical Sørensen similarity index, but it uses intermediate plots as steppingstones to calculate dissimilarities between plots that do not share species, which facilitates relating long compositional gradients to environmental variables (De'ath 1999).

We modeled the relationship between the NMDS axes and the set of topographic variables using linear mixed models (LMM) with gaussian distribution. Each of the two NMDS axes for each of the four plant groups was used separately as a response variable. We built models that included as explanatory variables HAND, drainage order and slope, and models that included only field measured topography as explanatory variable. To assess how the set of topographic variables explained the distribution of each individual species, we used generalized linear mixed models (GLMM) with binomial distribution (presence-absence data). Species occurrences were the response variables, and the quadratic forms of HAND, slope and Strahler's drainage order were the independent terms. We also built GLMMs that included only field measured topography as explanatory variable. For each individual species modelling, only transects within the same geological formation where a species had been registered were included in the species model to avoid overpredictions. We restricted our analysis to those species considered as frequent in the dataset, with at least 20 occurrences. Transect identity and transect affiliation to geological formation were set as random terms in all LMMs. The first aimed to account for the autocorrelation of sub-samples within transects; the second, to account for the marked differences in the environmental conditions of each geological formation. In GLMMs, only transect identity was set as a random term because the modelled species were rare in the three geological formations, so geological differences were not a relevant factor in the models.

In both community (LMM) and species-level models (GLMM), all variables were standardized by subtracting the mean and dividing by the standard deviation prior to the analyses to compare the effect sizes based on model

coefficients. For the models that contained HAND, slope and Strahler's order as variables, we applied a model selection procedure that started with a full model and then, models with different combination of the variables were compared using the *dredge* function of the R package MuMIn (Barton 2018). The best model was selected based on the Akaike Information Criteria (AIC). When more than one model had AIC < 2, the best model was determined as an average of their estimated standardized coefficients (Anderson and Burnham 2004), using the *model.avg* function of the R package MuMIn (Barton 2018). Model evaluation was done by comparing the model's AIC with a null model assuming no explanatory variables. Then, we evaluated the effect of the different variables in explaining either community composition (NMDS axes) or individual species occurrence in each model by comparing the magnitude and significance of the standardized beta coefficients of the final models. Coefficient values closer to 1 or -1 indicate stronger effect, whereas coefficient values closer to 0 indicate non-significant effects. The likelihood-ratio based pseudo- R^2 was reported individually for each model, with a maximum value of 1. LMM and GLMM using field measured topography as explanatory variable were also evaluated by comparing the model's AIC with a null model assuming no explanatory variable. All analyses were performed in the R statistical software (R Core Team 2020).

To evaluate the hierarchical importance of DEM-derived topographic variables in structuring plant communities in each geological formation, we used distance-based multivariate regression trees (MRT) (De'Ath 2002). We built MRT separately for each species group in each of the three geological surfaces (Solimões Formation, Içá Formation, and fluvial terrace). The two NMDS axes were set as dependent variables, and HAND, slope, and Strahler´s order as independent variables. MRTs were obtained by repeatedly splitting the observation units into two clusters that were determined by a break point in an environmental variable. Each split aimed to minimize the floristic differences between subunits in the same cluster, and at each level in the MRT, the variable that gives the minimum within-group sum of squared distance to the group mean was selected. This process was repeated with each sub-group of the previous step until each observation unit formed its own cluster.

We calculated dissimilarities using the Bray-Curtis index for occurrence data including all the species of each taxonomic group using the R package vegan (Oksanen *et al*. 2018). We used cross-validation to select the MRT with the smallest error (De'Ath 2002). The explained variation of the MRT is given by the residual error of the overall tree. MRTs were calculated using the functions of the R package mvpart (Therneau and Atkinson 2013).

RESULTS

Floristic composition

HAND was relevant to explain community composition of all plant groups except Melastomataceae (Figure 2a; Table 2). The effect was stronger for palms (b = -0.12) than for the other groups. Slope was only significant for pteridophytes (b = 0.04), and Strahler's drainage order was only significant for palms (b = 0.05). When NMDS axis 2 was the response variable (Figure 2b), HAND was still a significant variable for the same plant groups and had a strong effect for palms (b = -0.12). Strahler's drainage order was significant for palms (b = 0.10) and Zingiberales (b = -0.03). Slope had a significant effect for palms (b = -0.06) and Zingiberales (b = -0.03).

Individual species responses

Individual species responses to DEM-derived topographic variables were variable (Figure 3; Supplementary Material, Table S2). Pteridophytes (81%) and palms (80%) had the highest proportion of species that responded to the variation in HAND. Pteridophyte and Melastomataceae species responded mostly negatively, i.e., the probability of species occurrence decreased with increasing HAND values (Figure 3). For palm species, 55% had a positive response, i.e., species occurrence probability increased with increasing HAND values. Slope and Strahler's drainage order were significant in several models for all plant groups (Figure 3; Supplementary Material, Table S2). Model fit, as measured by the pseudo-R^2, varied from 0.05 – 0.45 in pteridophytes, 0.05 – 0.63 in Zingiberales, 0.05 – 0.45 in palms and 0.01 – 0.39 in Melastomataceae (Supplementary Material, Table S2). Out of the species restricted to a single geological formation, only one (*Calathea neblinense* - Zingiberales) had a positive relationship with HAND.

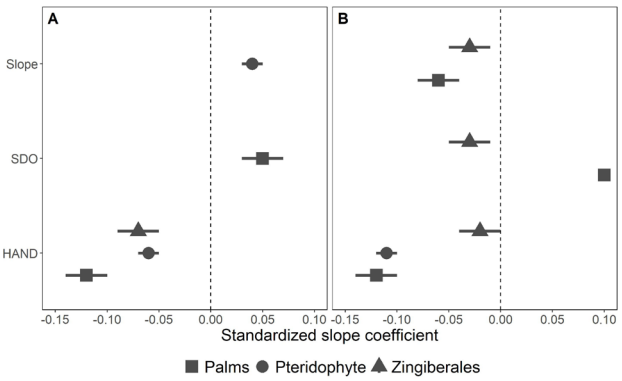

Figure 2. Output of the LMM for plant community data from the middle Juruá River (western Brazilian Amazon). Standardized slope coefficients and the standard error (horizontal bars) of the LMMs are shown for all variables used to model species occurrence with the NMDS axis 1 (A) and 2 (B). Coefficients different from zero are associated with significant effects. SDO = Strahler's drainage order.

Table 2. Summary of linear mixed models for plant communities along the middle Juruá River (western Brazilian Amazon) showing the results of model selection of the response of community composition (MDS1 and MDS2) to DEM-derived topographic metrics [HAND, slope and Strahler's drainage order (SDO)] and to field measured topography (Topo). The fit of the best models, alongside the null model assuming no explanatory variables (intercept-only), are shown for every response variable. Null models are shown separately for models with DEM-derived variables (Null) and for models with field measured topography (Null Topo). Response variables with null values are those for which the null model AIC was lower than for any model that included the variable.

Plant group	Response variable	Model	df	LogLink	AIC	ΔAICc
Pteridophytes	MDS1	HAND + Slope	6	-344.158	700.4	0
		Null	4	-355.615	719.3	18.88
		Topo	5	-324.770	659.6	0
		Null Topo	4	-355.615	719.3	59.67
	MDS2	HAND	5	-509.064	1028.2	0
		Null	4	-545.529	1099.1	70.91
		Topo	5	-492.247	994.5	0
		Null Topo	4	-545.529	1099.1	104.55
Zingiberales	MDS1	HAND + Slope	6	-344.158	700.4	0
		Null	5	-355.615	719.3	18.88
		Topo	5	-324.770	659.6	0
		Null Topo	4	-355.615	719.3	59.67
	MDS2	Null	4	-348.856	705.8	0
		Null Topo	4	-348.856	703.7	0
Palms	MDS1	HAND	5	-309.746	629.6	0
		Null	4	-316.312	640.7	11.11
		Topo	5	-299.290	608.7	0
		Null Topo	4	-316.312	640.7	32.02
	MDS2	Null	4	-348.856	705.8	0
		Null Topo	4	-348.856	705.8	0
Melastomataceae	MDS1	Null	4	-695.057	1326.1	0
		Topo	5	-657.789	1325.6	1.5
		Null Topo	4	-659.057	1326.1	0.52
	MDS2	Null	4	-798.735	1605.5	0
		Null Topo	4	-798.735	1605.5	0

Congruence with field measured topography

Overall, LMM and GLMM with field-measured topography as the sole explanatory variable had similar AIC values than models with DEM-derived topographic variables (Table 2, Supplementary Material, Figures S1, S2; Table S2). At the species level, the difference between the AICs, as assessed with an ANOVA, was not significant for any plant group (pteridophytes: p = 0.985, Zingiberales: p = 0.958, palms: p = 0.964, Melastomataceae: p = 0.927) (Supplementary Material, Figure S3).

Regression trees

Regression trees (Figure 4) showed that, in the river terraces, the main floristic differences for each species group were explained by drainage (pteridophytes, palms and Zingiberales, MRT residual errors = 0.87, 0.78 and 0.62, respectively) and slope (Melastomataceae, MRT residual error = 0.85). HAND was the variable that caused the main division of the MRT for the Içá Formation for all plant groups (MRT residual error: pteridophytes = 0.84, Zingiberales = 0.93, palms = 0.66, Melastomataceae = 0.94). In the Solimões Formation, the main division for all plant groups was associated with HAND (pteridophytes and Melastomataceae, MRT residual error = 0.88 and 0.96, respectively) and drainage (Zingiberales and palms, MRT residual error = 0.82 and 0.51, respectively).

DISCUSSION

HAND explained species composition of all plant groups, suggesting that this variable detected the influence of hydrological conditions as determined by topographic gradients. The underlying mechanisms to explain species distribution along topographic gradients are possibly related to species tolerance to desiccation or waterlogging. Desiccation is often associated with the distance to the water table on hilltops, while waterlogging is more common in areas close to the water table in local topographic bottomlands (Lopez and Kursar 1999; Parent *et al.* 2008; Oliveira *et al.* 2018; Fontes *et al.* 2020; Garcia *et al.* 2022).

Slope was also a significant variable to explain the floristic composition of pteridophytes (NMDS 1) and palms and

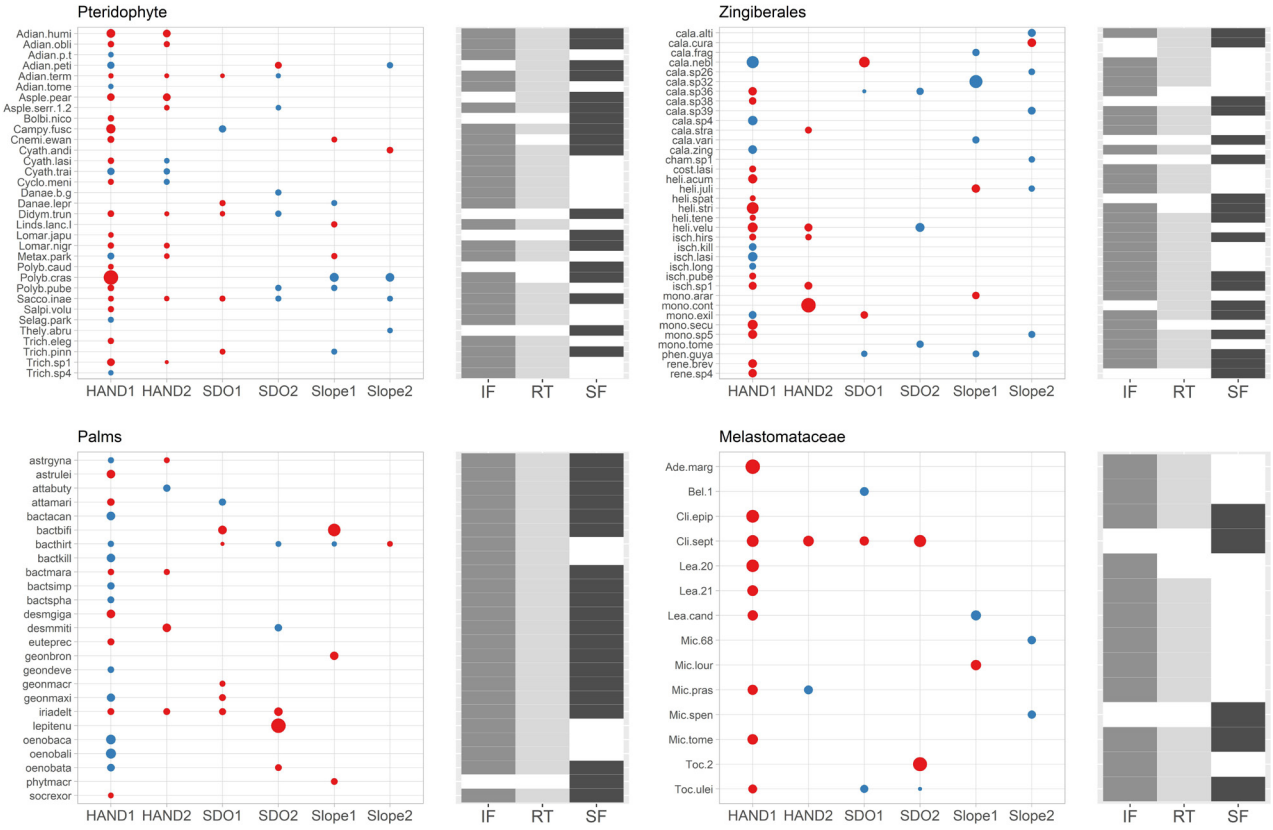

Figure 3. Output of GLMM for plant species occurrence along the middle Juruá River (western Brazilian Amazon). Dot size indicates the slope coefficient of the GLMM for all variables used to model species occurrence. Coefficients with higher variation are associated with stronger effects, either negative (decreasing species occurrence probability; red circles) or positive (increasing species occurrence probability; blue circles) of each variable. The tile plot to the right of each plot indicates in which geological formation each species was recorded (IF = Içá Formation; RT = river terraces; SF = Solimões Formation). SDO = Strahler's drainage order. The numbers 1 and 2 after each variable's name refer to the linear and squared terms, respectively. Species full names can be found in Table S2. This figure is in color in the electronic version.

Zingiberales (NMDS 2). The response of these plant groups to slope might reflect the strong slope gradient of the study area. Along topographic profiles, the slope angle indicates the capacity of the soil to retain moisture that infiltrates from precipitation (Rennó *et al.* 2008). On steep slopes, high lateral and sub superficial runoff diminish water infiltration, which is a limiting factor to plants that do not have deeper roots to anchor and access moisture from deeper soil layers (Fan *et al.* 2019). On the other hand, steep slopes do not accumulate as much litter as flat areas, so the lack of litter facilitates the establishment of seedlings of plants that do not have large nutrient reserves, such as the pteridophytes (Rodrigues and Costa 2012).

We found a significant effect of Strahler´s order in explaining floristic composition for palms (NMDS 1 and NMDS 2) and for Zingiberales (NMDS 2) in models where HAND also had a significant effect, suggesting that species responses to the modelled hydrological conditions were also related to the complementary effect of HAND in the gradient of drainage order formed along a watershed. Close to the watershed exit, bottomlands get inundated by rainwater because water infiltration is low when the soils are saturated due to the inundations of the large rivers (Miguez-Macho and Fan 2012). At the headwaters, the influence of low Strahler's order rivers on the soil saturation is dependent on terrain slope. While flat terrains can get frequently moist, in bottomlands of the areas with more pronounced slopes, the soil does not stay saturated after a rainfall because the small rivers have relatively low influence on soil saturation (Fan *et al.* 2013).

The occurrence of 57 % of the species in all plant groups was predicted using the DEM-derived variables. The models met some of our expectations. Species such as *Mickelia nicotianifolia*, *Campyloneurum fuscosquamatum* (pteridophytes), *Astrocaryum ulei* (palm) and *Clidemia epiphytica* (Melastomataceae) are commonly found in bottomlands and were correctly modelled to be negatively related to HAND, while *Oenocarpus bataua* (palm), commonly found on hilltops in western Amazonia, were correctly modelled to be positively related to HAND. Also, *Calathea altisssima* (ginger) has been described as common species on steep slopes and our models predicted its occurrence correctly. Habitat specialization related to topographic

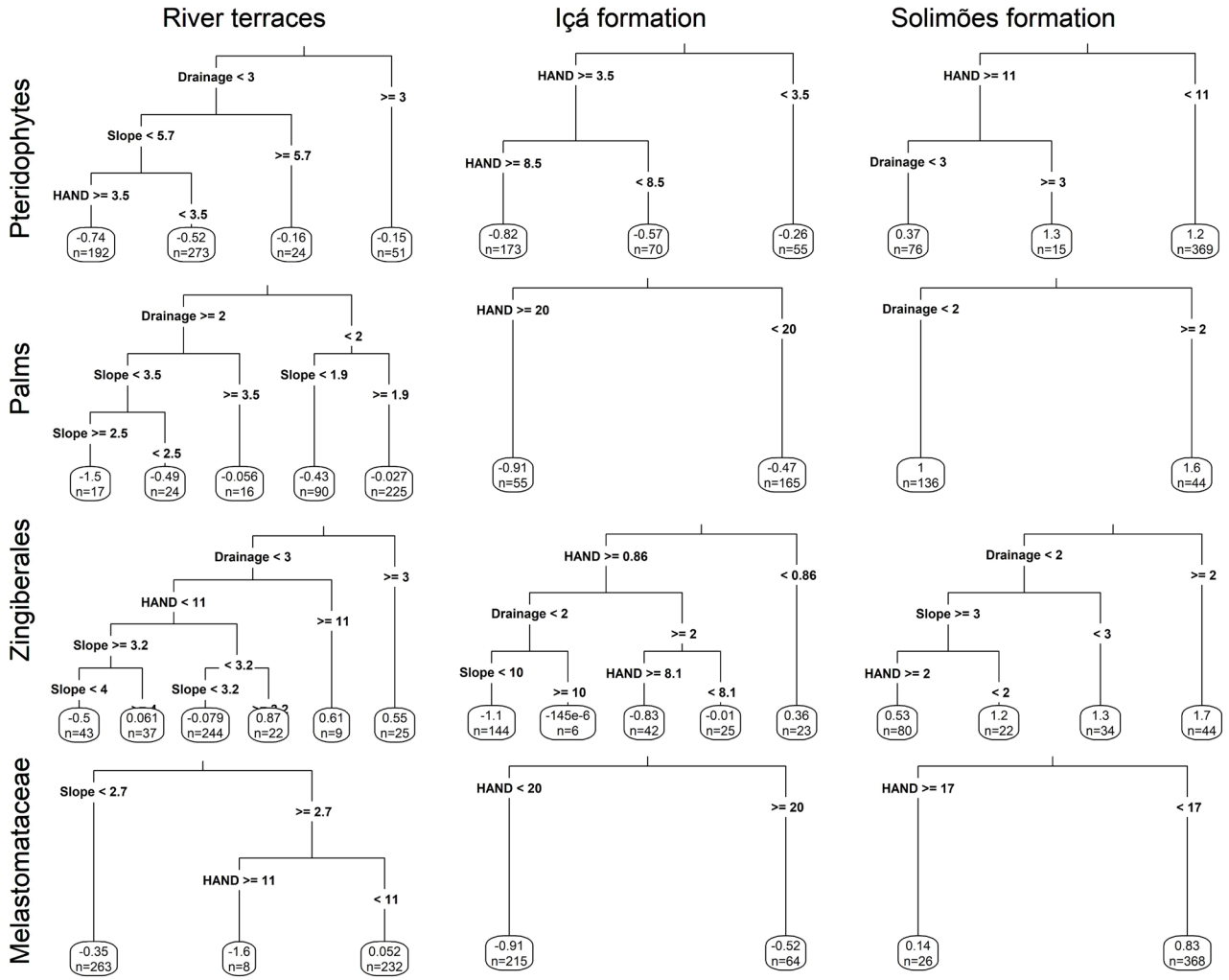

Figure 4. Distance-based multivariate regression trees showing clusters of transects established along 500 km of the middle Juruá River (western Brazilian Amazon). At each split of the tree, the dataset was divided into two according to the variables with higher importance value (upper nodes) in explaining differences in species composition. The value of each variable used to separate communities is shown. Branches could be subdivided several times. The number of subunits (n) that share similar species composition based on the Bray-Curtis similarity index is shown for each branch. Drainage = Strahler's drainage order.

position was reported before for many palms (Svenning 1999; Vormisto *et al.* 2004), pteridophytes (Tuomisto and Ruokolainen 1994; Tuomisto *et al.* 1995; 1998; Zuquim *et al.* 2012), Melastomataceae (Tuomisto and Ruokolainen 1994) and Zingiberales (Costa *et al.* 2005). These previous studies have used field-measured topographical variables, which accurately reflect slope and relative topographic position, but do not contain information about distance to water table and cannot be correlated across study areas. Our models using DEM-derived topography metrics were similar to models using field measured topography as explanatory variables at both community and species level, which is consistent with the idea that specialization to local topography might be related to species tolerance to water availability. However, as soil conditions were not evaluated in our study, the usefulness of DEM-variables as surrogates of field measured topography still requires further investigation.

Floristic patterns differed between geological formations. In the Içá Formation, HAND was the most important predictor of floristic composition for all the plant groups. This result may have been an effect of the Içá Formation being hillier, with a wider range of environmental conditions from lower to higher topographic positions relative to the Solimões Formation or the river terraces. Water availability likely changes for plants growing in different parts of this topographic gradient. Moreover, other soil conditions related to water availability may explain species distribution. Soils of the Içá Formation and river terraces in high topographic positions have coarser texture (Tuomisto *et al.* 2016) and may dry out faster than those in lower topographic levels. In the Solimões Formation and river terraces, finer sediments prevail,

and the water table is superficial, so that water availability is not a limiting factor for plants in dry periods. This would explain why drainage order was so important to explain floristic composition in the river terraces.

Applicability of DEM-derived variables

Our DEM-derived hydrological variables cannot be causally related to the physiological requirements of plants. Actual measurements of water table depth and soil moisture during sufficiently long periods of time would allow to characterize the role of hydrological conditions more accurately across topographic gradients in the different geological formations. However, long term field measurements across large areas in remote parts of Amazonia are logistically impracticable and of limited use for environmental monitoring (Frappart *et al.* 2019). Algorithms like HAND make it possible to remove the effect of regional topography and to retain only the local topography, so local hydrological conditions as estimated by HAND can be an efficient surrogate measure to describe hillslope hydrology (Fan *et al.* 2019) that can then be associated with species distribution. As the HAND eliminates the effect of absolute elevation values, the obtained results can be assumed to be quantitatively comparable to other parts of Amazonia.

The HAND algorithm has been used for ecological applications previously (Banon *et al.* 2019; Zuquim *et al.* 2021). Its applicability, however, is still limited by the need of validation points. HAND needs validation because the SRTM does not always accurately reflect topography due to complex interaction with the forest canopy, in a way that highly dissected valleys may remain unmapped (Valeriano *et al.* 2006). Our results show the usefulness of HAND and other DEM-derived metrics as predictors of floristic composition, but edaphic conditions need to be properly controlled to allow further interpretations. Thus, an assessment of the correlation between HAND and other environmental variables would help to disentangle its effect as a proxy for local hydrological conditions in Amazonian landscapes.

CONCLUSIONS

Our study showed that DEM-derived topographic variables can be useful to detect species preferences for local hydrological conditions defined by topographic gradients. The selected DEM-derived topographic variables were able to detect changes in floristic composition and individual species occurrences. The integration of topographic modelling of hydrological conditions in species modelling frameworks represents a significant advance in the mapping of Amazonian biodiversity, as knowledge on species tolerance to water- and soil-related environmental gradients is also critical for predicting how the viability and distribution of species might be affected by environmental changes.

ACKNOWLEDGMENTS

We are thankful to the people who made our expedition along the Juruá River possible and fruitful: the boat crew (José Rodrigues da Silva Filho, Radisvom Teixeira de Lima and Perla Maciel da Silva) and the local field assistants (especially José Francisco Gomes da Cruz). Research permits were granted by the Conselho Nacional de Desenvolvimento Científico e Tecnológico (CNPq) (process # 001693/2011-5), Centro Estadual de Unidades de Conservação (CEUC)/ Secretaria do Meio Ambiente e Desenvolvimento Sustentável do Estado do Amazonas (SDS) (authorization # 047/2011) and Sistema de Autorização e Informação em Biodiversidade (SISBIO) (license # 27998-3). This work was funded by the University of Turku Graduate School (grant to GMM), the Academy of Finland (grants # 139959 and 273737 to HT), Danish National Research Council (grant # 9040-00136B to HB), European Community (FP7-ENB-2007-1; EU Grant Agreement 212631 to HB), CNPq (fellowship to TE), Fundação de Amparo à Pesquisa do Estado de São Paulo (FAPESP) (project # 2016/13462–0, grant # 2016/18925-9 to LB), and Coordenação de Aperfeiçoamento de Pessoal de Nivel Superior (CAPES) (finance code 001). GMM acknowledges the postdoctoral grant from the Project SEP-CONACYT CB-2017-2018 (# A1-S-34563).

REFERENCES

Anderson, D.; Burnham, K. 2004. *Model Selection and Multi-Model Inference. v. 63*. 2nd ed. Springer-Verlag, New York, 488p.

Baldeck, C.A.; Tupayachi, R.; Sinca, F.; Jaramillo, N.; Asner, G.P. 2016. Environmental drivers of tree community turnover in western Amazonian forests. *Ecography,* 39: 1089–1099.

Balslev, H.; Luteyn, J.; Øllgaard, B.; Holm-Nielsen, L.B. 1987. Composition and structure of adjacent unflooded and floodplain forest in Amazonian Ecuador. *Opera Botanica,* 92: 37–57.

Banon, G.P.R.; Banon, G.J.F.; Villamarín, F.; Arraut, E.M.; Moulatlet, G.M.; Rennó, C.D.; *et al.* 2019. Predicting suitable nesting sites for the Black caiman (*Melanosuchus niger* Spix 1825) in the Central Amazon basin. *Neotropical Biodiversity,* 5: 47–59.

Banon, L. 2013. *Árvores de decisão aplicadas à extração automática de redes de dranagem*. Master´s dissertation, Instituto Nacional de Pesquisas Espaciais, Brazil. 87p. (http://urlib.net/8JMKD3MGP7W/3FB9RFE).

Barton, K. 2018. *Mu-MIn: Multi-model inference*. R package. (http://r-forge. r-project. org/projects/mumin/).

Cámara-Leret, R.; Tuomisto, H.; Ruokolainen, K.; Balslev, H.; Munch Kristiansen, S. 2017. Modelling responses of western Amazonian palms to soil nutrients. *Journal of Ecology,* 105: 367–381.

Campbell, D.G.; Daly, D.C.; Prance, G.T.; Maciel, U.N. 1986. Quantitative ecological inventory of terra firme and várzea tropical forest on the Rio Xingu, Brazilian Amazon. *Brittonia,* 38: 369–393.

Chadwick, K.D.; Asner, G.P. 2016. Tropical soil nutrient distributions determined by biotic and hillslope processes. *Biogeochemistry,* 127: 273–289.

Chauvel, A.; Lucas, Y.; Boulet, R. 1987. On the genesis of the soil mantle of the region of Manaus, Central Amazonia, Brazil. *Experientia,* 43: 234–241.

Costa, F.R.C.; Magnusson, W.E.; Luizao, R.C. 2005. Mesoscale distribution patterns of Amazonian understorey herbs in relation to topography, soil and watersheds. *Journal of Ecology,* 93: 863–878.

Costa, F.R.C.; Guillaumet, J.-L.; Lima, A.P.; Pereira, O.S. 2009. Gradients within gradients: The mesoscale distribution patterns of palms in a central Amazonian forest. *Journal of Vegetation Science,* 20: 69–78.

De'ath, G. 1999. Extended dissimilarity: a method of robust estimation of ecological distances from high beta diversity data. *Plant Ecology,* 144: 191–199.

Drucker, D.P.; Costa, F.R.C.; Magnusson, W.E. 2008. How wide is the riparian zone of small streams in tropical forests? A test with terrestrial herbs. *Journal of Tropical Ecology,* 24: 65–74.

Fan, Y.; Li, H.; Miguez-Macho, G. 2013. Global patterns of groundwater table depth. *Science,* 339: 940–943.

Fan, Y.; Clark, M.; Lawrence, D.M.; Swenson, S.; Band, L.E.; Brantley, S.L.; *et al*. 2019. Hillslope hydrology in global change research and earth system modeling. *Water Resources Research,* 55: 1737–1772.

Fontes, C.G.; Fine, P.V.A.; Wittmann, F.; Bittencourt, P.R.L.; Piedade, M.T.F.; Higuchi, N.; *et al*. 2020. Convergent evolution of tree hydraulic traits in Amazonian habitats: implications for community assemblage and vulnerability to drought. *New Phytologist,* 228: 106–120.

Frappart, F.; Papa, F.; Güntner, A.; Tomasella, J.; Pfeffer, J.; Ramillien, G.; *et al*. 2019. The spatio-temporal variability of groundwater storage in the Amazon River Basin. *Advances in Water Resources,* 124: 41–52.

Garcia, M.N.; Hu, J.; Domingues, T.F.; Groenendijk, P.; Oliveira, R.S.; Costa, F.R.C. 2022. Local hydrological gradients structure high intraspecific variability in plant hydraulic traits in two dominant central Amazonian tree species. *Journal of Experimental Botany,* 73: 939–952.

Gentry, A.H. 1988. Changes in plant community diversity and floristic composition on environmental and geographical gradients. *Annals of the Missouri Botanical Garden,* 75: 1–34.

Guimaraes, A.F.; de Souza, C.R.; Rosa, C.; Paulo dos Santos, J.; Teixeira, L.A.F.; Zanzini, L.P.; *et al*. 2021. Small-scale environmental variations drive vegetation structure and diversity in Amazon riverine forests. *Flora,* 283: 151916.

Haitjema, H.M.; Mitchell-Bruker, S. 2005. Are water tables a subdued replica of the topography? *Ground Water,* 43: 781–786.

Higgins, M.A.; Ruokolainen, K.; Tuomisto, H.; Llerena, N.; Cardenas, G.; Phillips, O.L.; *et al*. 2011. Geological control of floristic composition in Amazonian forests. *Journal of Biogeography,* 38: 2136–2149.

Hoorn, C.; Wesselingh, F. 2011. *Amazonia, Landscape and Species Evolution: A Look into the Past*. John Wiley & Sons, Chichester, 883p.

Jirka, S.; McDonald, A.J.; Johnson, M.S.; Feldpausch, T.R.; Couto, E.G.; Riha, S.J. 2007. Relationships between soil hydrology and forest structure and composition in the southern Brazilian Amazon. *Journal of Vegetation Science,* 18: 183–194.

Kahn, F.; de Castro, A. 1985. The palm community in a forest of central Amazonia, Brazil. *Biotropica,* 17: 210–216.

Karger, D.N.; Conrad, O.; Böhner, J.; Kawohl, T.; Kreft, H.; Soria-Auza, R.W.; *et al.* 2017. Climatologies at high resolution for the earth's land surface areas. *Scientific Data,* 4: 170122.

Lopez, O.R.; Kursar, T.A. 1999. Flood tolerance of four tropical tree species. *Tree Physiology,* 19: 925–932.

Miguez-Macho, G.; Fan, Y. 2012. The role of groundwater in the Amazon water cycle: 1. Influence on seasonal streamflow, flooding and wetlands. *Journal of Geophysical Research. Atmospheres,* 117: 1–30.

Moeslund, J.E.; Arge, L.; Bøcher, P.K.; Dalgaard, T.; Odgaard, M.V.; Nygaard, B.; *et al*. 2013. Topographically controlled soil moisture is the primary driver of local vegetation patterns across a lowland region. *Ecosphere,* 4: 1–26.

Moulatlet, G.M.; Costa, F.R.C.; Rennó, C.D.; Emilio, T.; Schietti, J. 2014. Local hydrological conditions explain floristic composition in lowland Amazonian forests. *Biotropica,* 46: 395–403.

Nobre, A.D.; Cuartas, L.A.; Hodnett, M.; Rennó, C.D.; Rodrigues, G.; Silveira, A.; *et al*. 2011. Height Above the Nearest Drainage – a hydrologically relevant new terrain model. *Journal of Hydrology,* 404: 13–29.

Oliveira, R.S.; Costa, F.R.C.; van Baalen, E.; de Jonge, A.; Bittencourt, P.R.; Almanza, Y.; *et al*. 2018. Embolism resistance drives the distribution of Amazonian rainforest tree species along hydro-topographic gradients. *New Phytologist*, 221:1457–1465.

Osher, L.J.; Buol, S.W. 1998. Relationship of soil properties to parent material and landscape position in eastern Madre de Dios, Peru. *Geoderma,* 83: 143–166.

Parent, C.; Capelli, N.; Berger, A.; Crèvecoeur, M.; Dat, J.F. 2008. An overview of plant responses to soil waterlogging. *Plant Stress,* 2: 20–27.

Poulsen, A.D.; Tuomisto, H.; Balslev, H. 2006. Edaphic and floristic variation within a 1-ha plot of lowland Amazonian rain forest. *Biotropica,* 38: 468–478.

R Core Team. 2020. *R: A language and environment for statistical computing. R Foundation for Statistical Computing*, Vienna, Austria. (http://www.R-project.org/).

Rennó, C.D.; Nobre, A.D.; Cuartas, L.A.; Soares, J.V.; Hodnett, M.G.; Tomasella, J.; *et al*. 2008. HAND, a new terrain descriptor using SRTM-DEM: Mapping terra-firme rainforest environments in Amazonia. *Remote Sensing of Environment,* 112: 3469–3481.

Rocchini, D.; Boyd, D.S.; Féret, J.-B.; Foody, G.M.; He, K.S.; Lausch, A.; *et al*. 2016. Satellite remote sensing to monitor species diversity: potential and pitfalls. *Remote Sensing in Ecology and Conservation,* 2: 25–36.

Rodrigues, F.R. de O.; Costa, F.R.C. 2012. Litter as a filter of emergence for herbaceous seedlings and sporophytes in central Amazonia. *Journal of Tropical Ecology,* 28: 445–452.

Schietti, J.; Emilio, T.; Rennó, C.D.; Drucker, D.P.; Costa, F.R.C.; Nogueira, A.; *et al*. 2014. Vertical distance from drainage drives floristic composition changes in an Amazonian rainforest. *Plant Ecology & Diversity,* 7: 241–253.

Strahler, A.N. 1957. Quantitative analysis of watershed geomorphology. *Eos, Transactions American Geophysical Union,* 38: 913–920.

Svenning, J.-C. 1999. Recruitment of tall arborescent palms in the Yasuní National Park, Amazonian Ecuador: are large treefall gaps important? *Journal of Tropical Ecology,* 15: 355–366.

Tuomisto, H.; Ruokolainen, K. 1994. Distribution of Pteridophyta and Melastomataceae along an edaphic gradient in an Amazonian rain forest. *Journal of Vegetation Science,* 5: 25–34.

Tuomisto, H.; Poulsen, A.D. 2000. Pteridophyte diversity and species composition in four Amazonian rain forests. *Journal of Vegetation Science,* 11: 383–396.

Tuomisto, H.; Poulsen, A.D.; Moran, R.C. 1998. Edaphic distribution of some species of the fern genus *Adiantum* in western Amazonia. *Biotropica,* 30: 392–399.

Tuomisto, H.; Ruokolainen, K.; Kalliola, R.; Linna, A.; Danjoy, W.; Rodriguez, Z. 1995. Dissecting Amazonian biodiversity. *Science,* 269: 63–66.

Tuomisto, H.; Moulatlet, G.M.; Balslev, H.; Emilio, T.; Figueiredo, F.O.G.; Pedersen, D.; *et al*. 2016. A compositional turnover zone of biogeographical magnitude within lowland Amazonia. *Journal of Biogeography,* 43: 2400–2411.

Tuomisto, H.; Van doninck, J.; Ruokolainen, K.; Moulatlet, G.M.; Figueiredo, F.O.G.; Sirén, A.; *et al.* 2019. Discovering floristic and geoecological gradients across Amazonia. *Journal of Biogeography*, 46: 1734–1748.

Valeriano, M.M.; Kuplich, T.M.; Storino, M.; Amaral, B.D.; Mendes Jr., J.N.; Lima, D.J. 2006. Modeling small watersheds in Brazilian Amazonia with shuttle radar topographic mission-90 m data. *Computers & Geosciences,* 32: 1169–1181.

Vormisto, J.; Tuomisto, H.; Oksanen, J. 2004. Palm distribution patterns in Amazonian rainforests: What is the role of topographic variation? *Journal of Vegetation Science,* 15: 485–494.

Wittmann, F.; Householder, E.; Piedade, M.T.F.; de Assis, R.L.; Schöngart, J.; Parolin, P.; *et al*. 2013. Habitat specifity, endemism and the neotropical distribution of Amazonian white-water floodplain trees. *Ecography,* 36: 690–707.

Zuquim, G.; Tuomisto, H.; Costa, F.R.C.; Prado, J.; Magnusson, W.E.; Pimentel, T.; *et al.* 2012. Broad scale distribution of ferns and lycophytes along environmental gradients in central and northern Amazonia, Brazil. *Biotropica,* 44: 752–762.

Zuquim, G.; Tuomisto, H.; Chaves, P.P.; Emilio, T.; Moulatlet, G.M.; Ruokolainen, K.; *et al*. 2021. Revealing floristic variation and map uncertainties for different plant groups in western Amazonia. *Journal of Vegetation Science,* 32: e13081.

RECEIVED: 05/01/2022
ACCEPTED: 16/06/2022
ASSOCIATE EDITOR: Eduardo Maeda

SUPPLEMENTARY MATERIAL (only available in the electronic version)

Moulatlet *et al.* The role of topographic-derived hydrological variables in explaining plant species distributions in Amazonia

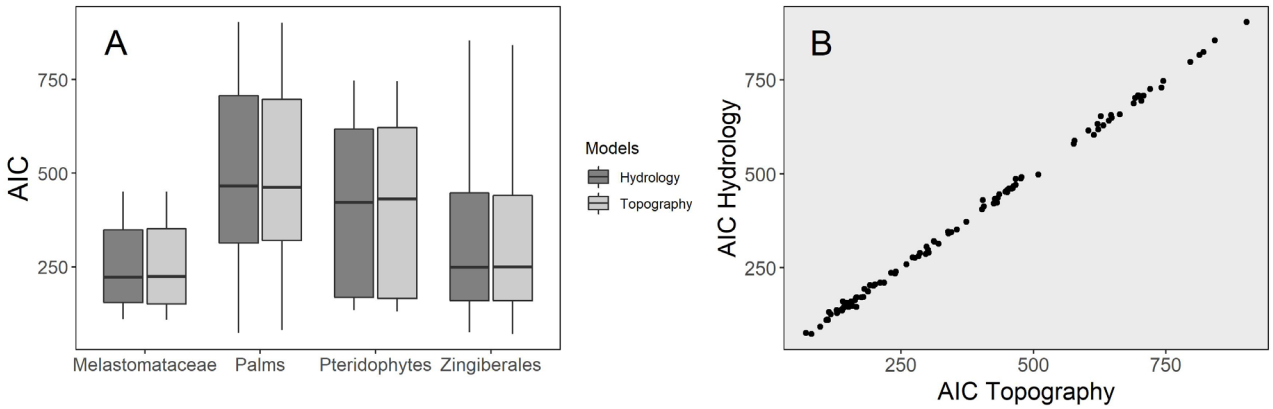

Figure S1. Comparison between generalized linear mixed models built at species-level with DEM-derived topographic metrics (Hydrology) and with field measured topography (Topography) from transects along the middle Juruá River (western Brazilian Amazon). A – Distribution of AIC values for each plant group; B – Comparison between AICs for each modelled species. Pearson's R = 0.99.

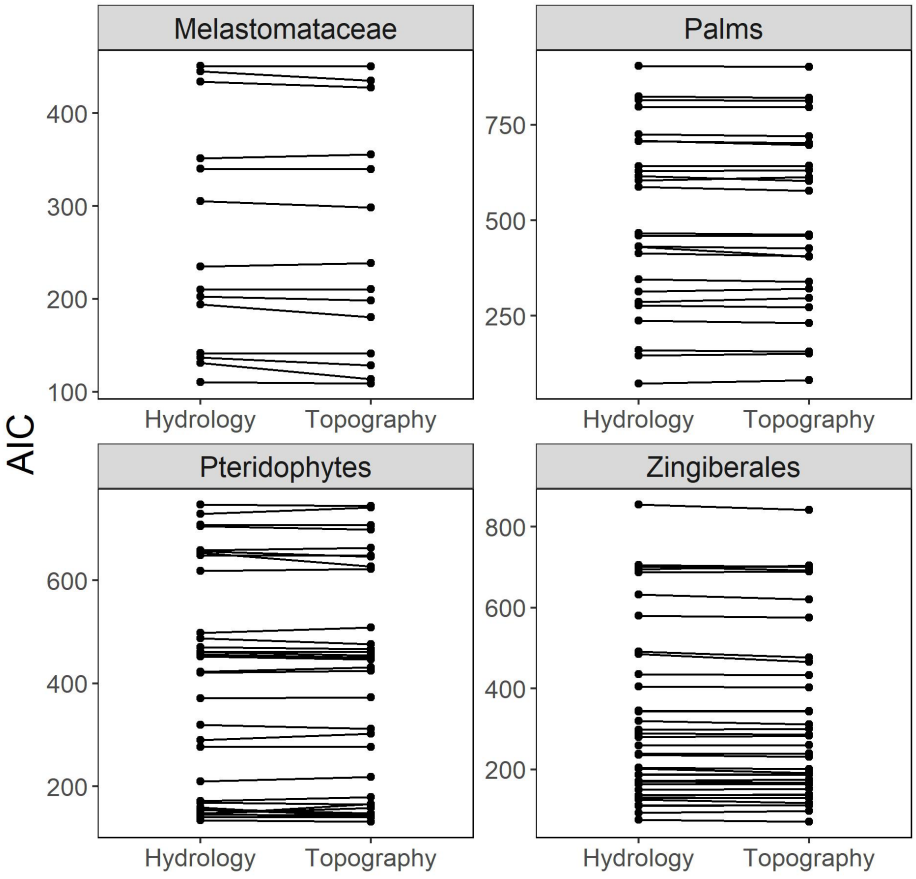

Figure S2. Comparison between generalized linear mixed models built at species-level with DEM-derived topographic metrics (Hydrology) and with field measured topography (Topography) for each species of each plant group sampled in transects along the middle Juruá River (western Brazilian Amazon). The results of Hydrological vs. Topographic models are connected for each individual species.

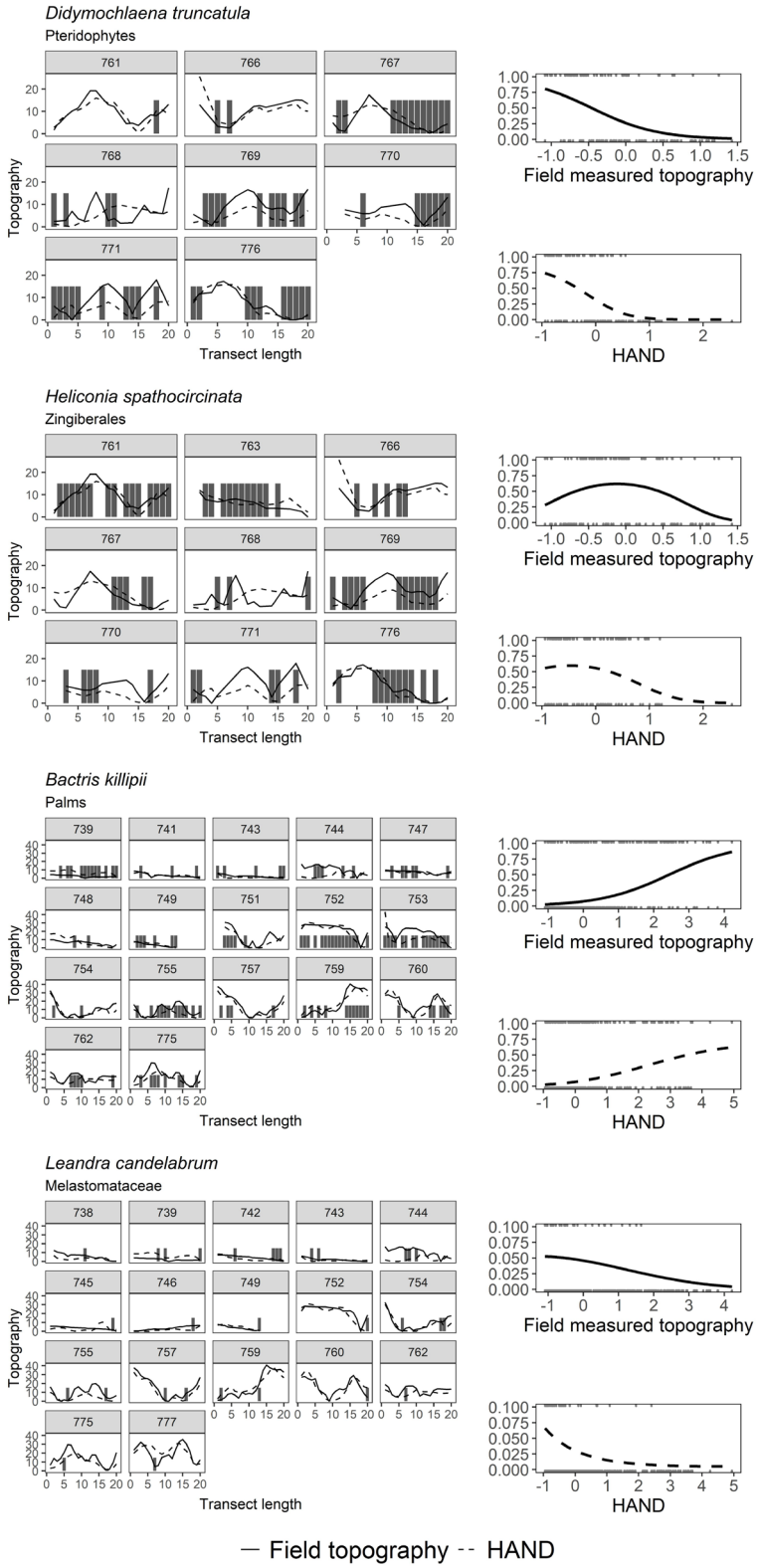

Figure S3. Presence of one selected species (vertical bars) of each plant group sampled in the set of transects along the middle Juruá River (western Brazilian Amazon). The transect (250 m total length) is divided in 20 subunits of 25 m each. Solid lines correspond to the field measured topographic profiles. Dashed lines correspond to the calculated HAND values. Species occurrence probabilities according to the field measured topography and to HAND are shown in the right column. Both variables are standardized by subtracting the mean and dividing by the standard deviation.

Table S1. Number of plant species used in each model and the corresponding number of transects and subunits within transects along the middle Juruá River (western Brazilian Amazon). Values within parenthesis indicate the number of species significantly associated to at least one hydrological variable in GLMM.

	Community level analysis			Species level analysis		
Plant group	**Species**	**Transects**	**Subunits**	**Species**	**Transects**	**Subunits**
Pteridophytes	170	58	1160	50 (33)	39	711
Zingiberales	115	32	632	60 (36)	39	711
Palms	62	33	660	39 (25)	39	711
Melastomataceae	149	58	1055	39 (14)	32	582

Table S2. Summary of generalized linear mixed models (GLMM) for individual plant species sampled in transects along the middle Juruá River (western Brazilian Amazon). Coefficients of each model (at logit scale) are shown with the respective standard errors (SE), p-values and pseudo-R^2. The numbers 1 and 2 after each variable's name refer to the linear and squared terms, respectively. AIC values are shown for the models with DEM-derived topographic variables (AIC DEM) and for the models with field measured topography (AIC Topo).

Plant group/species	**Species code**	**Variable**	**Coefficient**	**SE**	**p**	**AIC DEM**	**AIC Topo**	**Pseudo R^2**
Pteridophytes								
Adiantum humile	Adian.humi	HAND1	-57.78	20.44	0	290.6	302.1	0.298
		HAND2	-37.12	15.73	0.02			
Adiantum obliquum	Adian.obli	HAND1	-17.1	7.92	0.03	461.2	454.2	0.082
		HAND2	-13.74	6.81	0.04			
Adiantum paraense or *A. tuomistoanum*	Adian.p.t	HAND1	8.51	3.16	0.01	649.4	648	0.069
Adiantum petiolatum	Adian.peti	Slope2	15.6	7.54	0.04	134.5	131.1	0.128
		SDO2	-23.07	9.67	0.02			
		HAND1	28.88	6.67	0			
Adiantum terminatum	Adian.term	HAND1	-6.17	0.38	0	705.3	698.9	0.156
		HAND2	-4.05	0.49	0			
		SDO1	-3.19	0	0			
		SDO2	5.59	0	0			
Adiantum tomentosum	Adian.tome	HAND1	7.98	2.95	0.01	747.4	744.8	0.054
Asplenium pearcei	Asple.pear	HAND1	-33.68	10.91	0	157	147.3	0.214
		HAND2	-35.73	17.45	0.04			
Asplenium serratum	Asple.serr.1.2	SDO2	9.21	3.27	0	707.9	707.4	0.088
		HAND2	-8.96	4.02	0.03			
Bolbitis nicotianifolia	Bolbi.nico	HAND1	-18.55	6.95	0.01	160.2	140	0.193
Campyloneurum fuscosquamatum	Campy.fusc	SDO1	31.47	6.26	0	461.9	460.6	0.278
		HAND1	-71.07	22.74	0			
Cnemidaria ewanii	Cnemi.ewan	Slope1	-11.78	5.67	0.04	172.2	178.9	0.112
		HAND1	-22.93	5.66	0			
Cyathea andina	Cyath.andi	Slope2	-19.19	8.12	0.02	141.4	139.7	0.244
Cyathea lasiosora	Cyath.lasi	HAND1	-17.02	4.92	0	141.4	450.4	0.447
		HAND2	8.5	3.49	0.02			
Cyathea trailli	Cyath.trai	HAND1	29.7	12.57	0.02	209.9	218.4	0.443
		HAND2	18.18	8.92	0.04			
Cyclodium meniscioides	Cyclo.meni	HAND1	-12.45	4.89	0.01	422.7	431.2	0.217
		HAND2	12.5	4.07	0			
Danaea subgen. Arthrodanaea	Danae.b.g	SDO2	15.52	6.89	0.02	276.5	276.2	0.158

Table S2. Continued.

Plant group/species	Species code	Variable	Coefficient	SE	p	AIC DEM	AIC Topo	Pseudo R^2
Danaea leprieurii	Danae.lepr	Slope1	12.42	4.45	0.01	498	509	0.278
		SDO1	-15.16	5.55	0.01			
Didymochlaena truncatula	Didym.trun	SDO1	-7.55	0	0	147	143.2	0.347
		SDO2	15.41	0	0			
		HAND1	-19.74	0.01	0			
		HAND2	-5.12	0.01	0			
Lindsaea lancea var. lancea	Linds.lanc.l	Slope1	-16.9	6.53	0.01	618.5	622.3	0.217
Lomariopsis japurensis	Lomar.japu	HAND1	-8.34	3.72	0.02	155.1	144.7	0.19
Lomariopsis nigropaleata	Lomar.nigr	HAND1	-16.96	4.2	0	653.8	626.9	0.309
		HAND2	-11.79	3.69	0			
Metaxya parkerii	Metax.park	Slope1	-15.16	5.41	0.01	371.9	373.1	0.226
		HAND1	23.63	6.21	0			
		HAND2	-8.32	3.68	0.02			
Polybotrya caudata	Polyb.caud	HAND1	-9.66	4.34	0.03	169.9	165	0.184
Polybotrya crassirhizoma	Polyb.cras	Slope1	62.81	22.53	0.01	145.8	165.6	0.398
		Slope2	57.96	21.94	0.01			
		HAND1	-270.21	133.56	0.04			
Polybotrya pubens	Polyb.pube	Slope1	16.66	4.87	0	470.4	466.6	0.390
		SDO2	15.86	6.17	0.01			
		HAND1	-19.48	4.78	0			
Saccoloma inaequale	Sacco.inae	Slope2	11.06	3.7	0	658.5	663	0.265
		SDO1	-12.74	4.8	0.01			
		SDO2	12.86	3.78	0			
		HAND1	-11.51	4.13	0.01			
		HAND2	-7.86	3.5	0.02			
Salpichlaena volubilis	Salpi.volu	HAND1	-15.01	4.74	0	320	312.4	0.134
Selaginella parkeri	Selag.park	HAND1	13.08	3.78	0	420.7	425	0.122
Thelypteris abrupta	Thely.abru	Slope2	8.48	3.5	0.02	148.9	158	0.373
Trichomanes elegans	Trich.eleg	HAND1	-16.8	4.42	0	487.8	476.1	0.109
Trichomanes pinnatum	Trich.pinn	Slope1	12.59	4.75	0.01	729.5	741.6	0.276
		SDO1	-10.84	3.89	0.01			
Trichomanes sp. 1	Trich.sp1	HAND1	-36.98	0	0	452.3	446.8	0.271
		HAND2	-2.03	0	0			
Trichomanes sp. 4	Trich.sp4	HAND1	7.5	3.48	0.03	656.7	646.4	0.188
Zingiberales								
Calathea altissima	cala.alti	Slope2	15.74	5.68	0.01	694.1	703.8	0.316
Calathea curaraya	cala.cura	Slope2	-19.85	9.38	0.03	136.8	136.4	0.513
Calathea fragilis	cala.frag	Slope1	12.86	5.01	0.01	171.6	175.7	0.120
Calathea neblinense	cala.nebl	SDO1	-37.95	16.82	0.02	129	129.3	0.293
		HAND1	54.81	17.84	0			
Calathea sp. 26	cala.sp26	Slope2	9.15	4.47	0.04	171	166.4	0.293
Calathea sp. 32	cala.sp32	Slope1	66.29	24.3	0.01	93	97.2	0.3

Table S2. Continued.

Plant group/species	Species code	Variable	Coefficient	SE	p	AIC DEM	AIC Topo	Pseudo R^2
Calathea sp. 36	cala.sp36	HAND1	-18.56	7.21	0.01	163.9	162.8	0.086
		SDO1	3.42	0	0			
		SDO2	12.95	0	0			
Calathea sp. 38	cala.sp38	HAND1	-13.68	4.65	0	110.6	112	0.392
Calathea sp. 39	cala.sp39	Slope2	14.84	7.04	0.04	259.1	260.3	0.135
Calathea sp. 4	cala.sp4	HAND1	26.74	5.31	0	289.7	285.6	0.414
Calathea straminea	cala.stra	HAND2	-10.55	3.49	0	486.2	466.1	0.402
Calathea variegata	cala.vari	Slope1	11.46	5.33	0.03	136	138.5	0.269
Calathea zingiberina	cala.zing	HAND1	21.33	3.82	0	435.4	432.6	0.246
Chamaecostus sp. 1	cham.sp1	Slope2	8.68	3.37	0.01	126.7	117.2	0.255
Costus lasius	cost.lasi	HAND1	-10.59	4.93	0.03	491.6	477.4	0.054
Heliconia acuminata	heli.acum	HAND1	-24.47	11.86	0.04	239.5	240.1	0.064
Heliconia juruana	heli.juli	Slope1	-18.98	7.02	0.01	298.3	300.9	0.212
		Slope2	7.96	3.73	0.03			
Heliconia spathocircinata	heli.spat	HAND1	-6.48	3.14	0.04	203.6	191.1	0.075
Heliconia striata	heli.stri	HAND1	-50.69	23.17	0.03	186.5	188	0.406
Heliconia tenebrosa	heli.tene	HAND1	-7.45	3.11	0.02	855.1	841.9	0.168
Heliconia velutina	heli.velu	SDO2	22.96	7.49	0	405.5	402.6	0.422
		HAND1	-30.11	7.47	0			
		HAND2	-15.69	5.61	0.01			
Ischnosiphon hirsutus	isch.hirs	HAND1	-10.56	4.18	0.01	701.7	692	0.234
		HAND2	-8.49	3.61	0.02			
Ischnosiphon killipi	isch.kill	HAND1	14.21	5.71	0.01	188	187.1	0.08
Ischnosiphon lasiocoleus	isch.lasi	HAND1	26.97	12.45	0.03	205.1	200.7	0.533
Ischnosiphon longiflorus	isch.long	HAND1	10.68	3.12	0	633	200.7	0.13
Ischnosiphon puberulus	isch.pube	HAND1	-10.66	3.9	0.01	705.3	700.7	0.219
Ischnosiphon sp. 1	isch.sp1	HAND1	-15.82	7.28	0.03	579.8	575.7	0.208
		HAND2	-14.94	6.14	0.01			
Monophyllanthe araracuarensis	mono.arar	Slope1	-13.09	6.46	0.04	236.9	231.5	0.626
Monotagma contrariosum	mono.cont	HAND2	-88.59	33.05	0.01	149.8	152.1	0.28
Monotagma exile	mono.exil	SDO1	-13.6	6.4	0.03	345.2	344.8	0.286
		HAND1	14.75	5.03	0			
Monotagma secundum	mono.secu	HAND1	-30.37	11.46	0.01	76.4	70.3	0.555
Monotagma sp. 5	mono.sp5	Slope2	10.94	5.25	0.04	343.9	342.7	0.47
		HAND1	-22.74	8.79	0.01			
Monotagma tomentosum	mono.tome	SDO2	12.96	6.27	0.04	320.3	312.1	0.094
Phenakospermum guyanensis	phen.guya	Slope1	9.44	3.42	0.01	687.3	689.1	0.227
		SDO1	7.75	3.61	0.03			
Renealmia breviscapa	rene.brev	HAND1	-21.07	7	0	280.4	283	0.09
Renealmia sp. 4	rene.sp4	HAND1	-18.42	6.61	0.01	112.8	111	0.213
Palms								
Astrocaryum gynacanthum	astrgyna	HAND1	7.46	3.3	0.02	725.1	720.1	0.306
		HAND2	-6.47	2.75	0.02			

Table S2. Continued.

Plant group/species	Species code	Variable	Coefficient	SE	p	AIC DEM	AIC Topo	Pseudo R^2
Astrocaryum ulei	astrulei	HAND1	-21.45	6.95	0	588.1	577.1	0.275
Attalea butyracea	attabuty	HAND2	13.02	5.64	0.02	237.2	231.5	0.304
Attalea maripa	attamari	SDO1	12.61	4.16	0	603.9	613.8	0.181
		HAND1	-14.33	4.99	0			
Bactris acanthocarpa	bactacan	HAND1	23.07	5.11	0	413.4	406.1	0.223
	bactbifi	Slope1	-66.11	27.72	0.02			
Bactris bifida	bactbifi	SDO1	-22.17	9.37	0.02	286.9	296.6	0.444
Bactris hirta	bacthirt	HAND1	8.02	0.47	0	466.7	462.2	0.056
		Slope1	4.94	1.35	0			
		Slope2	-6.23	0.09	0			
		SDO1	-3.4	0	0			
		SDO2	6.88	0	0			
Bactris killipii	bactkill	HAND1	20.89	4.25	0	430.2	404.6	0.272
Bactris maraja	bactmara	HAND1	-8.72	3.61	0.02	816.1	813.4	0.213
		HAND2	-7.95	3.25	0.01			
Bactris simplicifrons	bactsimp	HAND1	13.18	3.67	0	628.7	631.6	0.053
Bactris sphaerocarpa	bactspha	HAND1	10.82	4.52	0.02	460.6	458.3	0.362
Desmoncus giganteus	desmgiga	HAND1	-21.45	10.36	0.04	313.3	320.8	0.026
Desmoncus mitis	desmmiti	SDO2	14	5.28	0.01	432.5	426.8	0.115
		HAND2	-21.6	8.52	0.01			
Euterpe precatoria	euteprec	HAND1	-11.72	3.14	0	824	821.1	0.201
Geonoma brongniartii	geonbron	Slope1	-20.51	9.32	0.03	346.3	338.8	0.447
Geonoma deversa	geondeve	HAND1	9.42	3.32	0	797.7	796	0.198
Geonoma macrostachys	geonmacr	SDO1	-7.04	3.32	0.03	707.4	701.9	0.324
Geonoma maxima	geonmaxi	SDO1	-11.28	3.9	0	708.9	697.6	0.309
		HAND1	19.04	4.07	0			
Iriartea deltoidea	iriadelt	SDO1	-11.45	4.16	0.01	641.5	642.3	0.207
		SDO2	-21.91	5.31	0			
		HAND1	-10.67	0	0			
		HAND2	-10.76	0	0			
Lepidocaryum tenue	lepitenu	SDO2	-96.38	35.05	0.01	73.5	81.2	0.393
Oenocarpus bacaba	oenobaca	HAND1	30.36	6.6	0	277.6	271.6	0.239
Oenocarpus balickii	oenobali	HAND1	34.08	11.98	0	146.3	151.4	0.093
Oenocarpus bataua	oenobata	SDO2	-10.13	4.21	0.02	615.7	603.4	0.371
		HAND1	15.28	5.47	0.01			
Phytelephas macrocarpa	phytmacr	Slope1	-10.13	4.02	0.01	160.9	156.2	0.306
Socratea exorrhiza	socrexor	HAND1	-6.08	2.89	0.04	904.3	901.9	0.104
Melastomataceae								
Adelobotrys marginata	Ade.marg	HAND1	-38.66	10.59	0	137.2	128.6	0.393
Bellucia sp. 1	Bel.1	SDO1	9.18	3.79	0.02	210.2	210.5	0.015
Clidemia epiphytica	Cli.epip	HAND1	-28.01	8.47	0	194.2	180.6	0.058

Table S2. Continued.

Plant group/species	Species code	Variable	Coefficient	SE	p	AIC DEM	AIC Topo	Pseudo R^2
Clidemia septuplinervia	Cli.sept	HAND1	-21.94	0.87	0	132.3	113.9	0.114
		HAND2	-16.3	0.02	0			
		SDO1	-10.77	0	0			
		SDO2	-23.49	0	0			
Leandra sp. 20	Lea.20	HAND1	-26.5	7.37	0	111	109.1	0.395
Leandra sp. 21	Lea.21	HAND1	-16.86	5.17	0	305.6	298.2	0.237
Leandra candelabrum	Lea.cand	Slope1	13.5	5.39	0.01	234.9	238.5	0.025
		HAND1	-15.02	6.8	0.03			
Miconia sp. 68	Mic.68	Slope2	7.73	3.38	0.02	340.6	339.6	0.058
Miconia lourteigiana	Mic.lour	Slope1	-14.74	0	0	202.8	198.2	0.04
Miconia prasina	Mic.pras	HAND1	-14.19	5.2	0.01	434.2	427.8	0.142
		HAND2	8.89	3.86	0.02			
Miconia spennerostachya	Mic.spen	Slope2	7.03	3.05	0.02	142.7	141.3	0.173
Miconia tomentosa	Mic.tome	HAND1	-15.48	5.92	0.01	451.1	450.3	0.166
Tococa sp. 2	Toc.2	SDO2	-35.87	13.73	0.01	351.6	355.6	0.101
Tococa ulei	Toc.ulei	HAND1	-8.92	3.87	0.02	445.4	435.3	0.01
		SDO1	6.74	0	0			
		SDO2	0.66	0	0			